Int. J. Electrochem. Sci., 12 **(2017)** 10239 – 10258, doi: 10.20964/2017.11.01

International Journal of
ELECTROCHEMICAL
SCIENCE
www.electrochemsci.org

A Facile Consistency Screening Approach to Select Cells with Better Performance Consistency for Commercial 18650 Lithium Ion Cells

Xiangming He[1,2], Gan Zhang[1], Xuning Feng[1,2], Li Wang[1,], Guangyu Tian[2], Minggao Ouyang[2]*

[1] Institute of Nuclear and New Energy Technology, Tsinghua University, Beijing 100084, P R China;
[2] State Key Laboratory of Automotive Safety and Energy, Tsinghua University, Beijing 100084, P R China
[*]E-mail: wang-l@tsinghua.edu.cn

Received: 6 June 2017 / *Accepted:* 29 August 2017 / *Published:* 12 October 2017

A battery pack for electric vehicles always contains many individual cells, but even more must be used for those made of 18650 cells. Cell-to-cell inconsistency can undermine the performance of a battery pack, and requires investigation before its formation. Traditional consistency screening approaches may have to check the electrochemical performance of the individual cells one after another, requiring plenty of time to filter the massive cells, whereas this study proposes a more efficient screening approach to select cells with better electrochemical consistency. By the proposed approach, the cells are connected in series and cycled with the same current, which makes performance consistency screening more reliable and more efficient. The weight, size, sealing, and electrochemical performances were tested and analyzed. These basic comparative results allow researchers and engineers to obtain a facile understanding of the inconsistency present in 18650 cell products. The inconsistency of cells from five manufacturers is quantitatively compared. Traditional screening approaches are based on the cell traits listed above, whereas the proposed approach in this study takes reduced time in cell screening by connecting 120 selected cells in series and cycling them simultaneously. Pack tests were conducted to verify the proposed consistency screening approach. The battery pack formed by cells with poor consistency selected by the proposed screening approach has a lower initial capacity after pack formation and shows faster capacity decay after cycling than one formed by cells with better consistency selected by the proposed screening approach, indicating that the proposed facile screening approach is effective.

Keywords: lithium ion cell; consistency; screening approach; series; battery

1. INTRODUCTION

Lithium ion cells are used to power today's electric vehicles[1,2]. Battery cells must form a pack to meet the high power output demand of electric vehicles[3,4]. Hundreds or even thousands of cells are required to form a battery pack[5]. Inconsistency exists among different cells[6,7], even for those from the same batch that are manufactured under similar environment. Any inconsistency among the cells can undermine the full performance of the battery pack[8]. For instance, the capacity of a battery pack will be less than the minimum capacity of the individual cells[9,10]. Furthermore, the inconsistency may grow during operation, resulting in an accelerated decay in the capacity of the battery pack[11,12]. Therefore, the cell inconsistency among the cells of a battery pack must be studied and well controlled.

Some research has been conducted to characterize and manipulate the inconsistency in a battery pack[13,14]. Generally, the characterizations focus on inconsistencies in the size, weight, capacity, resistance and other electrochemical characteristics of the cells. Raspa et al.[15] proposed using the discharge voltage, open circuit voltage, total capacity and Randle equivalent circuit model parameters as a basis and used the battery state of charge(SOC) changes to screen the cells. Kaizheng Fang et al.[16] proposed a method for screening cells based on the thermal behavior of the battery during charging. Jianbo Zhang et al.[17] used EIS and the equivalent circuit parameters to screen the cells. All these methods are based on the measurement of one cell at a time, which is time consuming. Muenzel et al.[18] proposed that a cell's construction can significantly affect its performance and lifetime. Devie and Dubarry[19] used the rate capability, the capacity ratio, and the Ohmic resistance to characterize cell-to-cell inconsistency. The many different characteristics that are used to study the cell-to-cell inconsistency can be coupled together, but the correlated research is complex and time-consuming without many effective results.

There are some available approaches to evaluate and control cell inconsistency[20]. Balancing, or 'equalization', is used to control the cell inconsistency within an acceptable range during the operation of the battery pack[21,22]. However, cell equalization can only recover the pack capacity to the minimum cell's capacity[23]. Therefore, cell-to-cell inconsistency must be reduced before pack formation. It is important to develop screening approach to filter the cell-to-cell inconsistency. Generally, cell inconsistency is characterized by specific tests using specific instruments[24,25]. The charge and discharge curves under different current rates contain rich information on the electrochemical features of the cell[26], and can thus be relied on to analyze the cell-to-cell inconsistency.

The 18650 cell is a typical type of cylindrical lithium ion battery, with a diameter of 18mm and a length of 65mm. The manufacturing of 18650 cells is mature with high automation, and reduced production costs. Therefore, the 18650 cell is favored by manufacturers of electric vehicles, e.g., Tesla Motors. However, because the capacity of the 18650 cell is low, many of them must be combined to form a battery pack. Therefore, a facile screening approach for large amounts of 18650 cells is meaningful and requires further study.

The screening methods of the manufacturers mainly focus on the measurement of the initial state parameters, including the initial capacity, the initial SOC, the initial internal resistance and the initial temperature. The screening methods of scientific research institutions mainly focus on measurements of the current state parameters, including the current capacity, the current EIS and so on. All the parameters mentioned above can only be measured cell by cell and thus, cannot be used to select cells with better performance consistency quickly and efficiently. Meanwhile, the effect of measurement deviation has not been fully considered, and sometimes the deviation requirements for consistency screening is even less than the measurement deviation. Therefore, this paper conducted a facile consistency screening approach to select cells with better consistency for commercial 18650 lithium ion cells. Selecting cells in series can ensure that the current is absolutely the same and effectively avoid the influence of measurement deviation on consistency screening. Additionally, the tester used in this experiment ensures that every cell is well ventilated, which can avoid the influence of temperature on the cell consistency measurements. The five selected manufacturers represent an average of the available manufactured cells, thereby making the basic comparative results useful for both researchers and engineers, allowing them to obtain a quick understanding of the inconsistency in current 18650 cell products. The weight, size, sealing, and electrochemical performances were tested and analyzed. The inconsistency of cells from the five manufacturers is quantitatively compared. All of the above experiments were conducted to verify that these batteries had a certain consistency before further screening. As the high voltage of the pack can only be economically achieved by connecting the cells in series, studying the consistency of cells in series is more important and practical than doing so in parallel. The proposed approach in this study connect 120 selected cells in series and charges and discharges them, which reduces the time required for cell screening. A facile screening approach was proposed to select a batch of cells with better consistency for further pack formation. The facile screening approach was validated through a pack cycling test.

2. EXPERIMENTAL

2.1. The battery cell

18650 cells from Company A, Company B, Company C, Company D and Company E were chosen for this study. Company A, Company C and Company D are global manufacturers, who are famous for the application of their products in 3C electronic devices and new energy vehicles. Company B and Company E are famous Chinese enterprises, who have stable market shares and advanced technologies. The quality of the 18650 cells produced by these five manufacturers may represent the current technology level of 18650 cell manufacturing. Therefore, the cell samples from these five manufacturers were selected to conduct a comparative study of the cell inconsistency. The battery cells from the five manufacturers are shown in Figure 1.

Figure 1. 18650 cell samples from five manufacturers

Table 1 summarizes the basic specifications offered by the five manufacturers.

Table 1 Nominal specifications offered by the five manufacturers

Cell manufacturer	Nominal voltage	Nominal capacity	Quantity under test
A	3.7V@0.2C	2600mAh	200
C	3.6V@0.2C	2600mAh	200
D	3.6V@0.2C	3000mAh	200
E	3.7V@0.2C	2600mAh	200
B	3.7V@0.2C	2200mAh	200

2.2. The test procedure

Several tests were designed and conducted to obtain detailed information about the inconsistencies of the cells, as shown in Figure 2. Weight and size check, sealing test, and performance test were conducted before a cell screening approach was proposed.

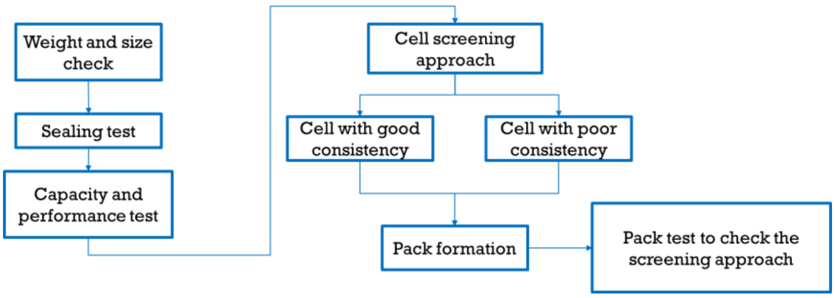

Figure 2. Flow of the test procedure in this study

2.3. Experimental design

2.3.1. Weight and size check

The specific energy and specific power of a cell are critical parameters, because the size and weight of the cell is limited onboard the electric vehicle. The cells were numbered from 1 to 200 for each manufacturer. The size and weight were measured using a caliper produced by Vernier® and using a balance produced by Mettler-Toledo®, respectively. The accuracy of the caliper is 0.02mm, whereas that of the balance is 10^{-5}g.

2.3.2. Sealing test

The cells may have to work under a variety of conditions in electric tools or vehicles. The sealing test is also important for preventing cell leakage, which may greatly affect the safety of cells because they can release flammable gases released.

The cells from the five manufacturers were put into a vacuum box for 24h with a vacuum pressure higher than 0.1MPa. The temperature was set to 20℃. After the sealing test, the mass loss of the cell should not be higher than 1mg, whereas the size expansion should not be higher than 0.2mm. Otherwise the cell is regarded as failing the sealing test, and is not tested further.

2.3.3. Capacity and performance characterization test

2.3.3.1. The charge and discharge test with 120 cells connected in series

As shown in Figure 3(a), the 120 randomly selected cells from all of the five manufacturers were connected in series. Therefore, all 120 cells can be charged and discharged simultaneously with precisely the same current, resulting in a quick test of the consistency of such a large number of 18650 cells. Compared with testing the cells in parallel, testing the cells in series requires a smaller current, but a higher voltage. The high voltage tests were conducted by a compatible Arbin tester, as shown in Figure 3(b).

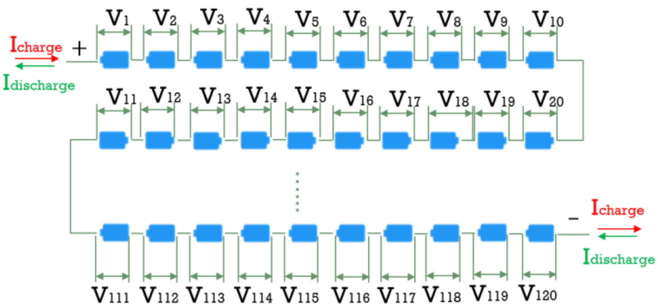

(a) 120 18650 cells connected in series

(b) Arbin tester with 120 cells connected in series

Figure 3. The charge and discharge test with 120 cells connected in series

The channels of the Arbin tester were connected in series to form the tester used for the 120-cell test. The terminals of the Arbin tester were connected tightly to avoid contact resistance. The 120-cell test started with a 10min static pause to observe the system's status. The 10min pause was followed by a 0.5C charge to 504V or any cell's voltage reached 4.2V. A 30min static pause was set before the cell was discharged at 1C until the total voltage reached 354V or any cell's voltage decreased to 2.95V. The voltages of the cells were recorded for another 30min after the discharge. The cut-off voltages were set as 4.2V and 2.95V to minimize the influence of the performance characterization test on the longevity of the cells, so that the good cells could be further integrated into a battery pack.

2.3.3.2. Charge and discharge test under different current rates

Through the approach proposed above, cells that represent the average characteristics of each of the five manufacturers can be obtained. The cells that represent the average characteristics of a battery batch are called the “average cells”. Then, 10 cells were selected from the average cells to compare the basic performance offered by each of the five manufacturers. The basic performance tests include the charge/discharge performance under variant current rates, the relationship between the SOC and the OCV, and the relationship between the SOC and the internal resistance. The batteries from the five manufacturers were discharged at 0.2C, 0.5C and 1C at 20℃, to obtain the capacity under different discharge rates. After the discharge tests, the cells were charged at 0.2C by a CC-CV profile to 4.2V with static pause for 1h afterwards. The resistance and the OCV at 100% SOC were evaluated using an internal resistance tester. Then, the cell was further discharged by 10% SOC to 90% SOC at 0.2C, and the resistance and OCV at 90% were evaluated again using the internal resistance tester. The test was repeated with a depletion of 10% SOC at each step, to measure fully the internal resistance and the OCV from 0% to 100% SOC.

2.3.4. The cell screening approach

Figure 4 shows the steps for the proposed facile screening approach. As mentioned in the introduction, the study of cells in series is more important and practical. Thus, 120 cells were randomly selected from 200 samples from each manufacturer. According to the test approach described in Sec. 2.3.3.1, the 120 cells were connected in series. The charge and discharge curves at 0.5C charging and 1C discharging were obtained.

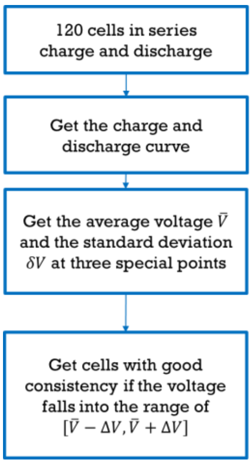

Figure 4. The facile screening approach for cell inconsistency

Based on the normal charging and discharging mechanism, the polarization of the cells becomes more obvious at the end of charging and discharging tests, so the internal resistance difference between the cells is also notable at these points. We relied on the notable characteristics at these points to design our quick cell screening approach. By observing the entire charge-discharge curve, we can conclude that the curve is consistent in a majority of the cases, and there is only significant inconsistency at the end of charging, at end of discharging and 30min pause after the end of discharging. The facile screening approach was applied by analyzing the characteristics at three selected characteristic points, including the voltage at end of charging, the voltage at the end of discharging, and the voltage after 30min pause after the end of discharging. The cells with better consistency were selected according to the statistics of the three selected characteristic points. The average voltage $\bar{V}$ and the standard deviation ΔV of the three selected points were analyzed. Within the range of $[\bar{V}-\Delta V, \bar{V}+\Delta V]$, the cells that have better consistency can be figured out. If all the characteristic voltages at the selected points fall into the range of $[\bar{V}-\Delta V, \bar{V}+\Delta V]$, the cell is regarded to have good consistency.

2.3.5. Pack test to check the proposed screening approach

To verify the effectiveness of the facile screening approach of cell consistency, 20 average cells with better consistency and 20 cells with worse consistency were selected and connected in series to form two battery packs. The cells used for pack test was chosen from D company. As the consistency of cells from D company is the best compared with other four companies before screening, we chose the cells from D company to verify the approach. If the cells from company D can verify this approach, cells from the other four companies can also verify this approach. Cycling tests were designed to investigate the capacity decay of the two battery packs. As shown in Figure 5, an Arbin tester was utilized to cycle the battery pack consisting of 20 screened cells in series using current rates of 0.5C for charging and 2C for discharging at 25℃. After 50 cycles, the capacity decays of the 20-cell packs were analyzed to verify the effectiveness of the proposed screening approach.

Figure 5 The pack test setup for verification of the facile screening approach

3. RESULTS AND DISCUSSION

3.1. Weight and size check

The weight of cells from the five 18650 manufactures are ordered as follows:

$$\text{Weight: D>E>A>C>B} \tag{1}$$

As the cells from Company D have the highest capacity(3000mAh), the weight of the Company D cell is the heaviest. On the contrary, the cells from B have the lightest weight. The weight consistencies are compared in Table 2 and Figure 6(a).

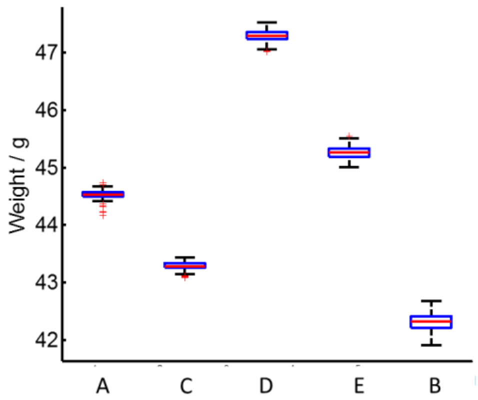

(a) Boxplot of the weights

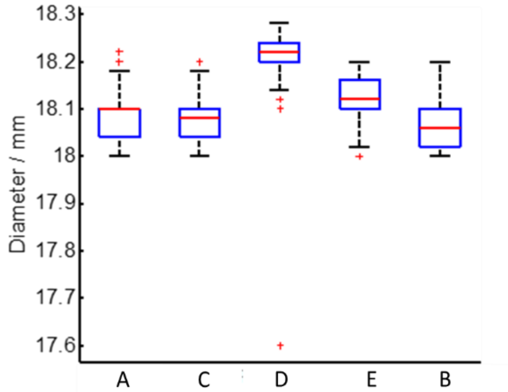

(b) Boxplot of the diameters

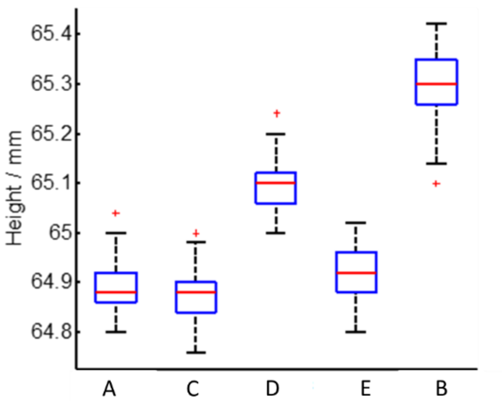

(c) Boxplot of the heights

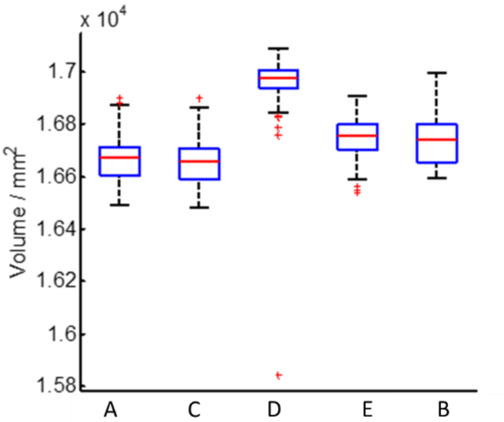

(d) Boxplot of the volumes

Figure 6. Boxplot comparing the inconsistency of the weights and sizes of the cells from the five manufacturers

Table 2. The statistics of the weight for 18650 cells from each manufacture

	A	C	D	E	B
Maximum weight/g	44.73	43.44	47.51	45.56	42.67
Minimum weight/g	44.17	43.08	47.01	45.01	41.92
Average weight/g	44.53	43.29	47.29	45.27	42.32
Standard deviation/g	0.073	0.067	0.101	0.107	0.142

Considering the standard deviation of the cell weight, the consistency of the weight from each of the five manufacturers can be ordered as follows:

$$\text{Standard deviation of weight: } C<A<D<E<B \quad (2)$$

The diameters D of the five manufactures' 18650 cells all exceed 18mm, within a range of 18.06mm-18.22mm as listed in Table 3 and shown in Figure 6(b). The oversized diameters may affect the integration of cells into packs. The height H of these batteries is within the range of 64.88mm-65.30mm, as listed in Table 4 and shown in Figure 6(c). The standard deviation of the diameter and the height were marked as ΔD and ΔH, respectively.

Table 3. The statistics of the diameter for 18650 cells from each manufacture

	A	C	D	E	B
Maximum diameter/mm	18.22	18.20	18.28	18.20	18.20
Minimum diameter/mm	18.00	18.00	17.60	18.00	18.00
Average diameter *D*/mm	18.08	18.08	18.22	18.12	18.06
Standard deviation ΔD/mm	0.048	0.046	0.052	0.038	0.048

Table 4. The statistics of the height for 18650 cells from each manufacturer

	A	C	D	E	B
Maximum height/mm	65.04	65.00	65.24	65.02	65.42
Minimum height/mm	64.80	64.76	65.00	64.80	65.10
Average height *H*/mm	64.89	64.88	65.10	64.92	65.30
Standard deviation ΔH/mm	0.051	0.049	0.047	0.054	0.061

The volume V_{ol} of the cells can be calculated by Eqn. (3), and the statistics of the cell volumes are derived in Table 5 and shown in Figure 6(d). For inconsistency in the cells' sizes, the quality of the cells from Company E is the best because it has the lowest standard deviation in volume. Although cells from Company D seem to have a centralized distribution in the boxplots shown in Figure 6, the number of exotic cells that fall outside of this average range is larger than that for any other company. Therefore, the standard deviation for the volume of cells from Company D is the highest among those of the five manufacturers.

Through testing and analyzing the quality, diameter, height and volume of all the cells, we can conclude that these cells have a good exterior consistency. Although the parameters of the cells from each manufacturer differ slightly, they are all within the deviation range, which means that further screening of the cells can proceed using the approach proposed above.

$$V_{ol} = \frac{\pi}{4} \cdot D^2 \cdot H \tag{3}$$

Table 5. The statistics of the volume for each manufacturer's 18650 cell

	A	C	D	E	B
Maximum volume/mm^2	1.690×10^4	1.690×10^4	1.709×10^4	1.691×10^4	1.699×10^4
Minimum volume/mm^2	1.649×10^4	1.648×10^4	1.584×10^4	1.654×10^4	1.660×10^4
Average volume V_{ol}/mm^2	1.666×10^4	1.665×10^4	1.697×10^4	1.675×10^4	1.674×10^4
Standard volume ΔV_{ol} /mm^2	87.7	87.0	96.0	71.4	89.4

3.2. Sealing test

The results of the sealing test are listed in Table 6. All the samples for Company E passed the sealing test, indicating that Company E had the best design for sealing the cells.

Table 6. Sealing test results

	A	C	D	E	B
Failure rate	0.5%	0.5%	0.5%	0%	1%
Failure terms	weight	weight	size	/	weight

3.3. Capacity and performance characterization test

3.3.1. The charge and discharge test with 120 cells connected in series

The 120 cells connected in series were numbered in order.

Figure 7 and Figure 8 illustrate the 0.5C charge curve and the 1C discharge curve for the cell from the five manufacturers, respectively. The number of the cell with the highest/lowest voltage are marked in Figure 7 and Figure 8.

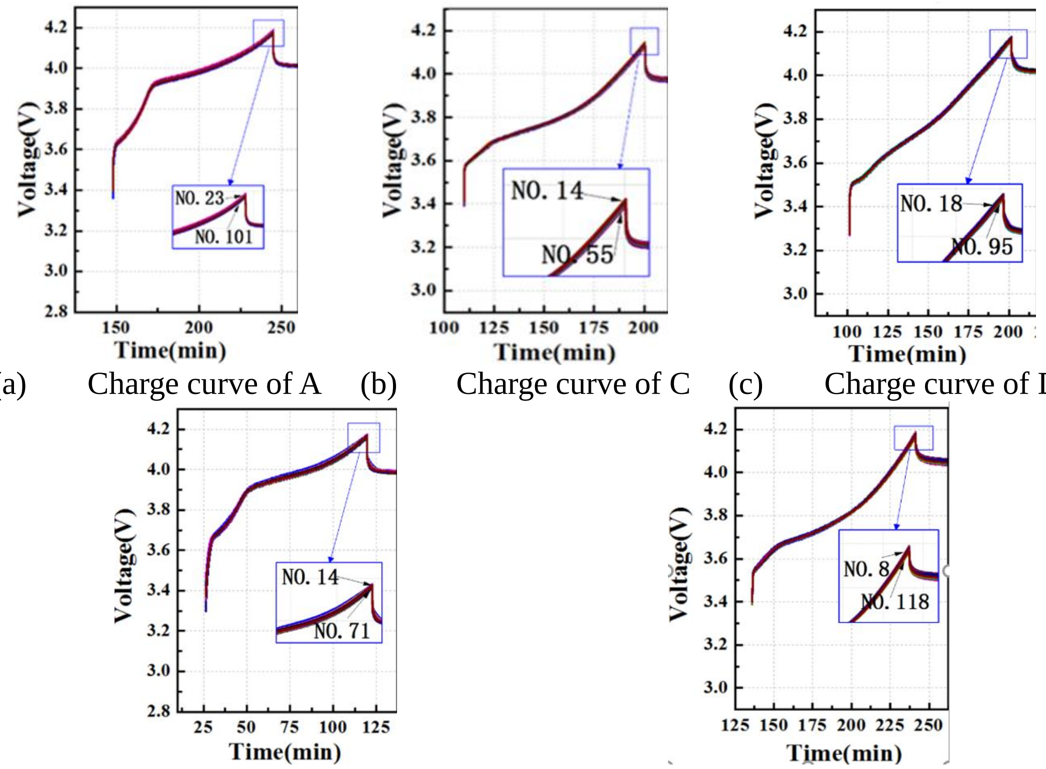

(a) Charge curve of A (b) Charge curve of C (c) Charge curve of D

(d) Charge curve of E (e) Charge curve of B

Figure 7. Charge curves of the individual cells in the 120-cell pack

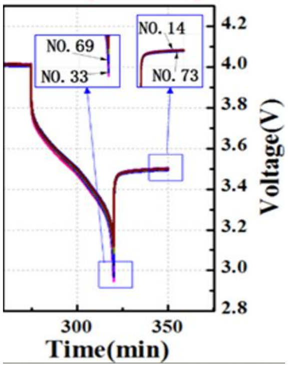

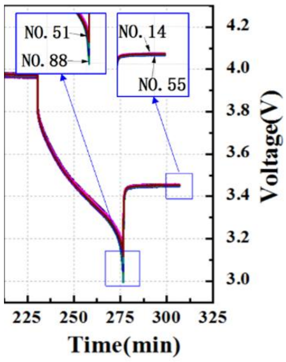

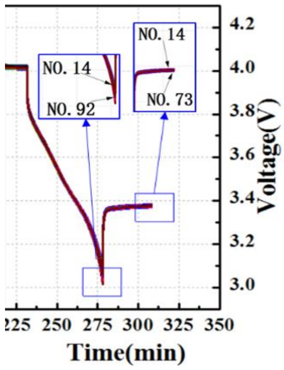

(a) Discharge curve (c) Discharge curve (e) Discharge curve
(b) of A (d) of C (f) of D

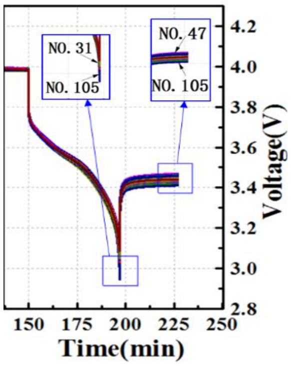

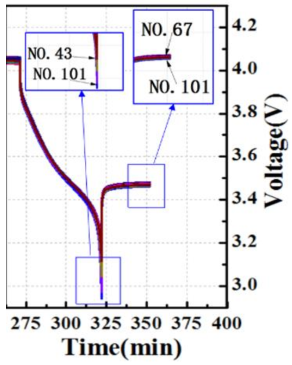

(g) Discharge curve of E (h) Discharge curve of B

Figure 8. Discharge curves of the individual cells in the 120-cell pack

Table 7. The maximum voltage difference D_V at the three selected points

	A	C	D	E	B
End of charge, $D_{V,\text{ end of discharge}}$ / mV	19.7	23.7	19.2	18.5	24.6
End of discharge, $D_{V,\text{ end of charge}}$ / mV	207.0	175.3	101.6	193.3	253.4
30min after discharge, $D_{V,\text{ 30min after discharge}}$ / mV	10.2	11.5	13.7	58.3	18.2

Table 7 shows the maximum voltage difference D_V at the three selected points for the cell samples of the five manufacturers. The maximum voltage difference at the end of discharge, $D_{V,\text{ end of discharge}}$, is the largest, whereas that at 30min after the discharge, $D_{V,\text{ 30min after discharge}}$, is the smallest, as shown in Eqn. (4).

$$D_{V,\text{ end of discharge}} > D_{V,\text{ end of charge}} > D_{V,\text{ 30min after discharge}} \quad (4)$$

The average voltage at the end of discharge, $\overline{V}_{EOD}$, reflects the resistance at 0% SOC and the depth of discharge for the cell samples. The $\overline{V}_{EOD}$for the five manufacturers are compared in Figure 9. The cells from Company D have the lowest $\overline{V}_{EOD}$, indicating the resistance at 0% SOC is the lowest for the cells from Company D compared with those of the other four manufacturers. The order of the $\overline{V}_{EOD}$ of the samples is as follows:

$$\overline{V}_{EOD}: \text{D(3.06V)< A=E(3.07V)<C=B(3.11V)} \quad (5)$$

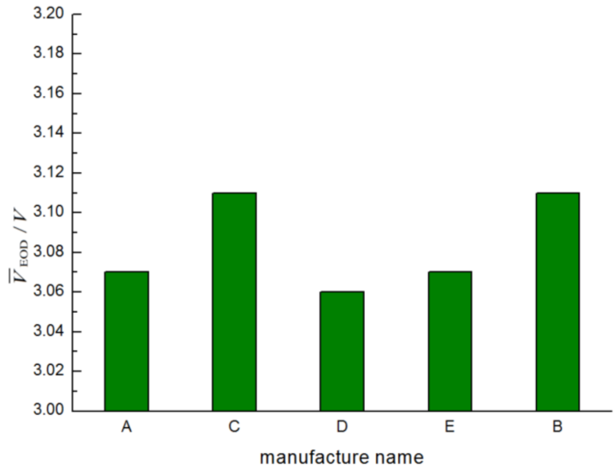

Figure 9. The average voltage at the end of discharge, $\overline{V}_{EOD}$, for the five manufacturers

The maximum voltage differences at the end of discharge, $D_{V,\ \mathrm{end\ of\ charge}}$, are compared in Figure 10. The cells from D have the smallest $D_{V,\ \mathrm{end\ of\ charge}}$. And the order of the $D_{V,\ \mathrm{end\ of\ charge}}$ from different manufacturers is as follows:

$D_{V,\ \mathrm{end\ of\ charge}}$: D(101.64mV)<C(175.3mV)<E(193.3mV)<A(207mV)< B(253.4mV) (6)

The average voltage $\overline{V}$ and the standard deviation ΔV of the three selected points can reflect the consistency of a cell batch, and are collected in Table 8 The standard deviation ΔV (measured in mV) is normalized into a percentage called δV using Eqn. (7).

$$\delta V = \Delta V / \overline{V} \times 100\% \qquad (7)$$

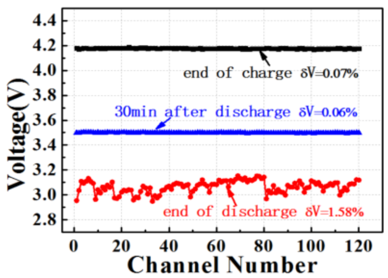

(a) Voltage and standard deviation of A

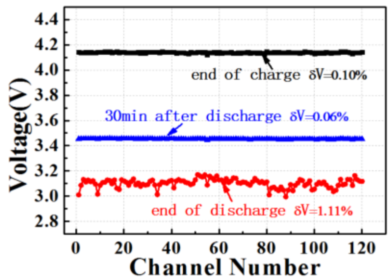

(b) Voltage and standard deviation of C

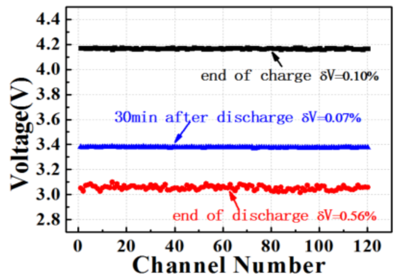

(c) Voltage and standard deviation of D

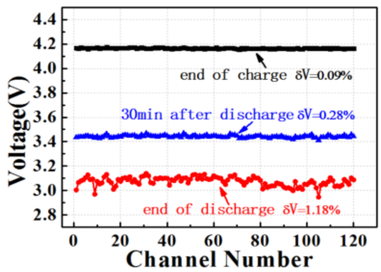

(d) Voltage and standard deviation of E

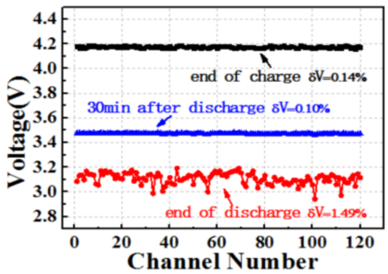

(e) Voltage and standard deviation of B

Figure 11. Voltage statistics the at the three selected points for the five manufacturers before screening

Table 8

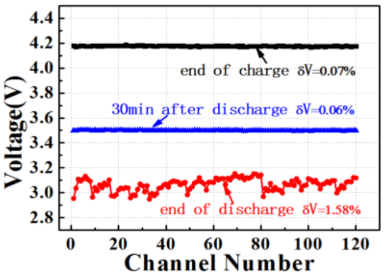

(f) Voltage and standard deviation of A

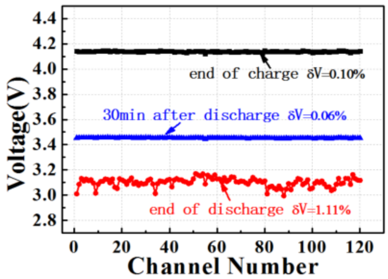

(g) Voltage and standard deviation of C

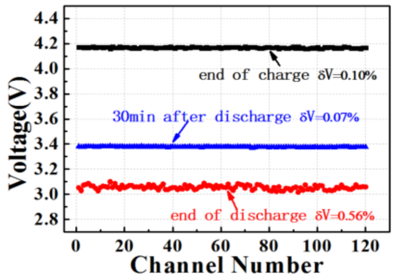

(h) Voltage and standard deviation of D

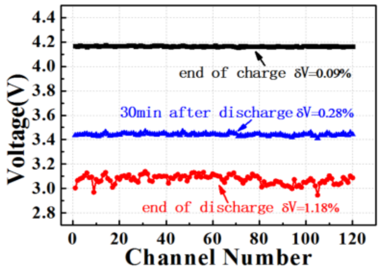

(i) Voltage and standard deviation of E

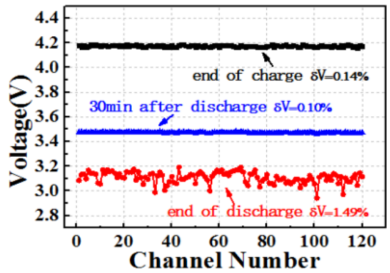

(j) Voltage and standard deviation of B

Figure 11. Voltage statistics the at the three selected points for the five manufacturers before screening

Table 8 shows the average voltage $\bar{V}$ and the standard deviation ΔV & δV of the three selected points for different cell samples before screening. Detailed voltage information for individual cells at these points is shown in Figure 11, with the relative standard deviation δV marked. The highest δV occurred for the voltage at the end of discharge. The order of the normalized standard deviation δV for the five manufacturers is shown in Eqn. (8). The cells from D have the best consistency when comparing the δV at the end of discharge.

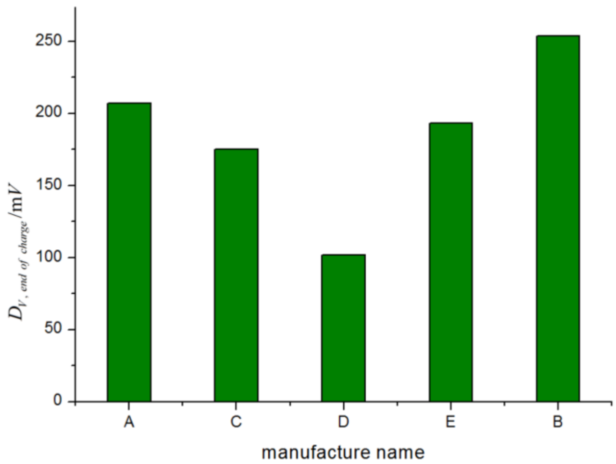

Figure 10. Maximum voltage differences at the end of discharge, $D_{\mathrm{V,\ end\ of\ charge}}$, for the five manufacturers

$$\delta V \text{ End of Discharge: D(0.56\%)<C(1.11\%)<E(1.18\%)<B(1.49\%)<A(1.58\%)} \tag{8}$$

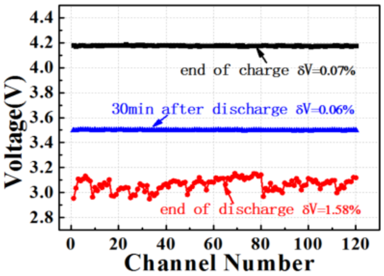

(k) Voltage and standard deviation of A

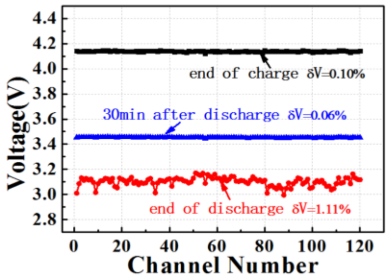

(l) Voltage and standard deviation of C

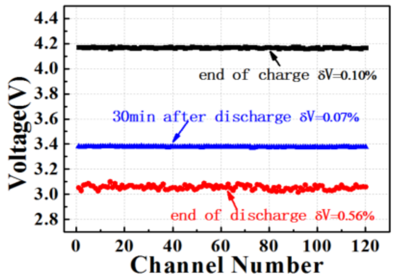

(m) Voltage and standard deviation of D

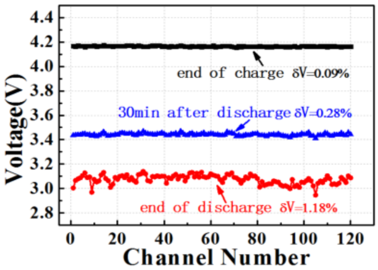

(n) Voltage and standard deviation of E

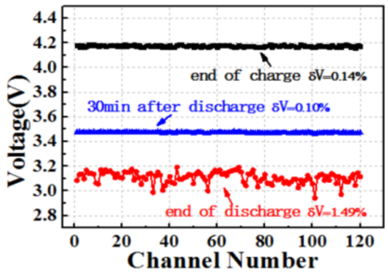

(o) Voltage and standard deviation of B

Figure 11. Voltage statistics the at the three selected points for the five manufacturers before screening

Table 8. Average voltage and standard deviation of the three selected points for the cell samples before screening

		A	C	D	E	B
End of charge	$\bar{V}$ / V	4.18	4.14	4.17	4.16	4.18
	ΔV / mV	19.7	23.7	19.2	18.5	24.6
	δV /%	0.07	0.10	0.10	0.09	0.14
End of discharge	$\bar{V}$ / V	3.06	3.10	3.06	3.07	3.11
	ΔV / mV	205.8	175.3	85.2	193.3	249.8
	δV /%	1.58	1.11	0.56	1.18	1.49
30min after discharge / mV	$\bar{V}$ / V	3.50	3.45	3.38	3.44	3.47
	ΔV / mV	10.2	11.5	13.7	58.3	18.2
	δV /%	0.06	0.06	0.07	0.28	0.10

3.3.2. Charge and discharge test under different current rates

Average cells were chosen from those whose voltages at the all three of the selected points were in the range of $[\bar{V} - \Delta V, \bar{V} + \Delta V]$. The average cells were tested using the profile proposed in Sec. 2.3.3.2.

Figure 12 illustrates the discharge capacity under different current rates at 20℃. The discharge capacities of the different cells display identical trends considering their discharge current rates. Although the nominal discharge capacity is asserted to be 2600mAh for the cells from Company A, Company C and Company E, the discharge capacities for all of these cells are lower than the nominal value. The cell from Company E has the largest discharge capacity among the three.

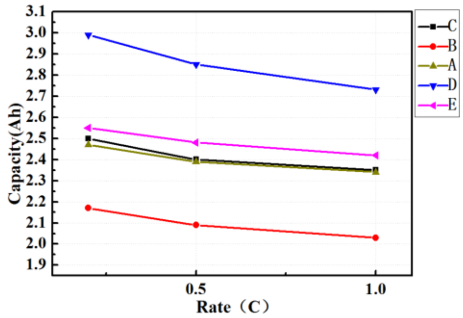

Figure 12. The discharge capacity under different current rates at 20℃

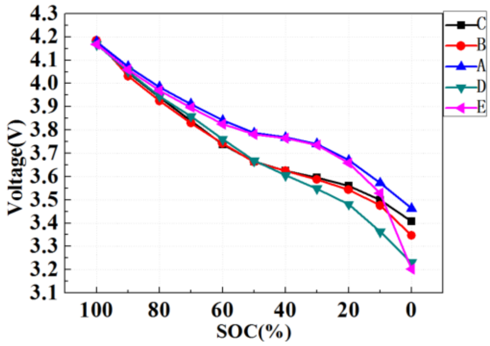

Figure 13. OCV-SOC diagram of the cell samples for the five manufacturers

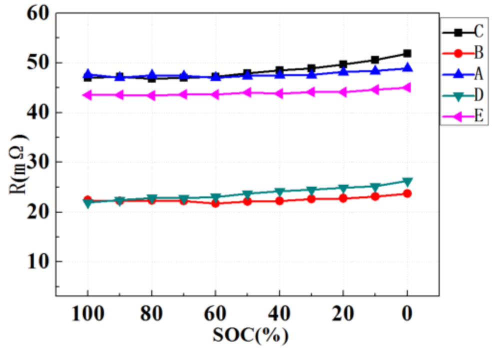

Figure 14. R-SOC diagram of the cell samples for the five manufacturers

Figure 13 shows the OCV-SOC diagram and Figure 14 shows the R-SOC diagram for the selected cells from the five manufacturers. As shown in Figure 13, the discharge voltage for the cells from Company A and Company E are higher than that from the other three manufacturers, indicating that the cells produced by Company A and Company E have a high power density. As shown in Figure 14, the cells with a capacity of 2600mAh (cells from Company A, Company C and Company E)have resistances at variant SOCs that are higher than that of the other two manufacturers. The cells from Company D and Company B have similar resistances, but the nominal capacity of the cell from Company D is 3000mAh, whereas that of Company B is 2200mAh.

3.4. The cell screening result

As proposed in Sec. 2.3.4, the cell screening approach selects cells that have voltages at the three selected points in the range of $[\bar{V}-\Delta V, \bar{V}+\Delta V]$. Eqn. (9) defines the screening approach in mathematical equations, where V_x denotes the characteristic voltage at the three selected points (end of charge, end of discharge, and 30min after discharge). If V_x at any of the three selected points is outside of $[\bar{V}-\Delta V, \bar{V}+\Delta V]$, the correlated cell is kicked out from the good-consistency batch.

$$(\bar{V}-\Delta V) \le V_x \le (\bar{V}+\Delta V) \tag{9}$$

ΔV was defined as the standard deviation of the corresponding characteristic voltages. The number of cells left in the good-consistency batch after screening cells from each of the five manufacturers was collected in Table 9. When the screening thresholds is set as $[\bar{V}-\Delta V, \bar{V}+\Delta V]$, C looks to be the best manufacturer, with the highest proportion of cells that are judged to have good consistency. Nevertheless, when the screening threshold expands to $[\bar{V}-2\Delta V, \bar{V}+2\Delta V]$ or even $[\bar{V}-3\Delta V, \bar{V}+3\Delta V]$, all of the cell samples from E fall into the screening range.

Table 9. The percentage of cells left in the good-consistency batch with variant screening thresholds

Screening threshold	A	C	D	E	B
$[\bar{V}-\Delta V, \bar{V}+\Delta V]$	61.7%	72.5%	63.3%	70.0%	70.0%
$[\bar{V}-2\Delta V, \bar{V}+2\Delta V]$	74.2%	82.5%	73.3%	100%	74.2%
$[\bar{V}-3\Delta V, \bar{V}+3\Delta V]$	91.7%	91.7%	91.7%	100%	94.2%

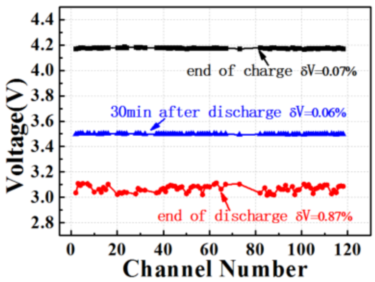

(a) Voltage and standard deviation(after screening) of A

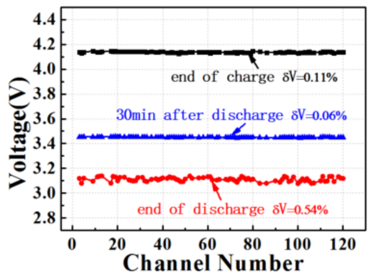

(b) Voltage and standard deviation(after screening) of B

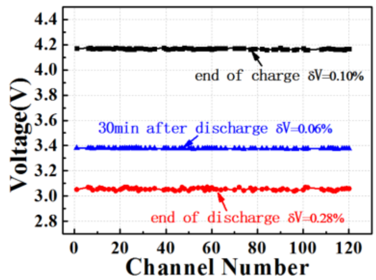

(c) Voltage and standard deviation(after screening) of D

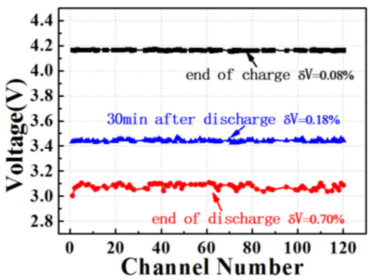

(d) Voltage and standard deviation(after screening) of E

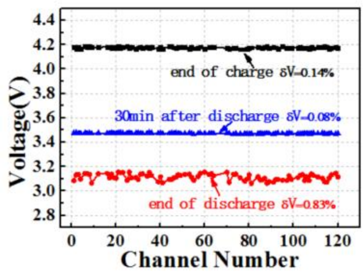

(e) Voltage and standard deviation (after screening) of B

Figure 15. Voltage statistics at the three selected points for the five manufacturers after screening

To form cell modules, we select $[\bar{V}-\Delta V, \bar{V}+\Delta V]$ as the screening range. All the cells that are out of the screening range were removed from the good-consistency batch. The cells left in the batch after the screening have a smaller standard deviation ΔV and δV.

Figure 15 shows the statistics of the voltages at the three selected points for the five manufacturers after the screening, and collects the average voltage and standard deviation of the three selected points for different cell samples after the screening. Compared with that before screening, the normalized δV is smaller, indicating that the consistency of the battery improved after screening. Therefore, this screening approach is effective.

Table 10. Average voltage and standard deviation of the three selected points for different cell samples after screening

		A	C	D	E	B
End of charge	$\bar{V}$ / V	4.18	4.14	4.17	4.16	4.18
	ΔV / mV	19.7	23.7	17.9	19.2	23.8
	δV /%	0.07	0.11	0.10	0.08	0.14
End of discharge	$\bar{V}$ / V	3.07	3.11	3.06	3.07	3.06
	ΔV / mV	95.3	61.9	32.8	68.1	91.6
	δV /%	0.87	0.54	0.28	0.70	0.83
30min after discharge / mV	$\bar{V}$ / V	3.50	3.45	3.38	3.44	3.47
	ΔV / mV	10.2	11.5	9.3	33.8	15.3
	δV /%	0.06	0.06	0.06	0.18	0.08

3.5. Pack test to check the screening approach

To verify further the utility of this screening approach, pack tests were conducted with 20 selected cells connected in series. One pack consists of 20 cells selected with good consistency (characteristic voltage in $[\bar{V} - \Delta V, \bar{V} + \Delta V]$), and another pack consists of 20 cells with poor consistency (characteristic voltage out of $[\bar{V} - \Delta V, \bar{V} + \Delta V]$). The two battery packs were cycled separately to observe the capacity decay and evaluate the validity of the proposed screening approach.

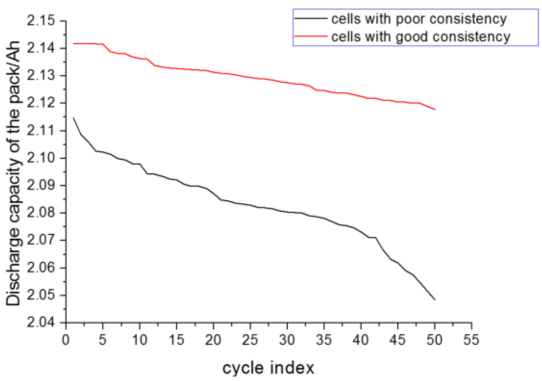

Figure 16. Capacity decay for the battery pack, one with good consistency, the other with poor consistency

Figure 16 shows that the initial capacity of the pack with poor consistency is 1.3% lower than that of the pack with good consistency. After cycling for 50 cycles, the capacity loss was 3.1% for the pack with poor consistency, but only 1.1% for the pack with good consistency. The decays of the battery packs indicate that the proposed screening approach is effective for quickly filtering cells with better consistency for pack formation.

3.6 Further discussion on the proposed cell screening approach

As those approaches mentioned in the papers [15,17,18] are based on the measurement of the cells one after another, we proposed to connect the cells in series and cycle them with a same current, which makes performance consistency screening more reliable and more efficient. The use of $[\bar{V} - \Delta V, \bar{V} + \Delta V]$ box as a simple and criterion also improves the screening efficiency, comparing with the approach using neural network model as in [15].

Pack tests as in Sec. 3.5 were also conducted to verify the proposed screening approach of cell inconsistency. The capacity of the battery pack is lower than that of individual cells and decays faster with cycles as in [27]. The battery pack with worse cell consistency has lower capacity than that with better cell consistency. Moreover, the capacity of the battery pack with worse cell consistency will decrease faster than that with better cell consistency, as indicated in [8].

Furthermore, some basic electrochemical characterizations were checked to validate the cell inconsistency after screening by the proposed approach, including the self-discharge rate and the discharge capacity under different current rates at 20℃. The results are listed in Table 11.

Randomly select 2 cells that have been selected out by the proposed approach from each company and charge them to their full capacity at 0.2C and 20℃. After that monitor the OCV every ten days. Thirty days later, discharge all cells to 2.75V and acquire the rest capacity and calculate the self-discharge rate. The results listed in Table 11 indicate that the capacity decay of these cells is approximately 98% after 30 days. However, the test standard required by the company instructions is less than 10% capacity decay in 30 days, indicating that the screening approach is capable to filter good cells from the gross set.

Table 11. The decay of OCV and capacity for cells after screening

	Full capacity state OCV（V）			Charge/discharge capacity(mAh)		
	OCV（after 10days）	OCV（after 20days）	OCV（after 30days）	Charge capacity	Discharge capacity（after 30days）	Discharge capacity（after 30days）/Charge capacity
C-131	4.15	4.12	4.12	2499	2458.9	98.4%
C-132	4.15	4.12	4.12	2494.7	2455.6	98.4%
A-124	4.15	4.14	4.14	2463.3	2433	98.8%
A-125	4.15	4.14	4.14	2466.2	2431.6	98.6%
B-23	4.15	4.13	4.13	2200.1	2163.7	98.3%
B-26	4.15	4.13	4.12	2207	2175.5	98.6%
D-149	4.15	4.13	4.12	2977.6	2937.1	98.6%
D-151	4.15	4.13	4.12	2978.3	2933.9	98.5%
E-132	4.15	4.14	4.13	2527.5	2486.9	98.4%
E-133	4.15	4.13	4.13	2551.6	2523.6	98.9%

Randomly select 2 cells that have been selected out by the proposed approach from each company and charge them to their full capacity at 0.2C and 20℃. Rest for an hour, and discharge them at 0.2C, 0.5C or 1C. The capacities at different discharge rates of the screened cells are much better than the that required in the company instructions (0.5C/0.2C>95%, 1C/0.2C>90%), as listed in Table 12.

Table 12. The discharge capacity at different current rates for cells after screening

Current	C-114	C-111	B-12	B-16	A-116	A-117	D-107	D-114	E-83	E-88
0.2C Charge	2.50	2.50	2.17	2.17	2.47	2.46	2.99	2.99	2.56	2.55
0.5C Discharge	2.40	2.40	2.09	2.09	2.39	2.39	2.86	2.84	2.49	2.48
0.5C/0.2C	96%	96%	96.%	96.%	96.%	97.%	95.%	95.%	97.%	97.%
1C Discharge	2.35	2.34	2.03	2.03	2.34	2.34	2.74	2.72	2.42	2.42
1C/0.2C	94%	93.%	93.%	93.%	94.%	95.%	91.%	91.%	94.%	94.%

All the results shown in Table 11 and 12 are much better than the standard requirements in the company instructions, indicating that the proposed approach in the manuscript not only meets the requirements of traditional screening approaches, but also fulfils the purpose of fast screening a large number of cells.

4. CONCLUSIONS

This paper proposes a facile consistency screening approach and provides a comparative study of the inconsistency for commercial 18650 lithium ion cells from five manufacturers. The inconsistency of the cells from the five manufacturers has been comprehensively compared, considering the weight, size, electrochemical performance, etc. The cell from Company C performs best in controlling the weight consistency for their 18650 products, whereas the cell from Company E is the best in controlling the volume consistency.

Three selected characteristic points, including the voltage at the end of charge, the voltage at the end of discharge, and the voltage 30min after discharge, were used to judge the consistency of the electrochemical performances of cells from different manufacturers. The cells from Company D and Company E seem to have better electrochemical performances than those from the other three.

The average voltage $\bar{V}$ at the three selected characteristic points and the standard deviation ΔV were used to help screen the cells for better consistency. If all three of the characteristic voltages at the three selected points fall in the range of $[\bar{V} - \Delta V, \bar{V} + \Delta V]$, the cell is regarded as having good consistency with others and represents the average electrochemical performances of cells from the same batch. A screening approach is proposed to select cells with better consistency using this heuristic. A pack test was conducted to verify this facile screening approach of cell inconsistency. The battery pack formed by cells with poor consistency has a lower initial capacity after pack formation and displayed faster capacity decay after cycling than that with good consistency, in indicating that the facile screening approach is effective.

This study shows that the proposed facile consistency screening approach can provide high performance consistency while reducing screening time.

Future work will focus on the influence of the temperature distribution on the electrochemical inconsistency of the cells. Cycling work is continuing to investigate the mechanism of the inconsistency evolution in battery pack considering degradation.

ACKNOWLEDGEMENTS
This work is supported by the National Natural Science Foundation of China (Grant No. U1564205 and No. 20901046), the Ministry of Science and Technology of China (Grant 2013CB934000, No. 2014DFG71590, No. 2016YFE0102200), and the Beijing Municipal Program (Grant No. YETP0157).

References

1. M. Hu, J. Wang, C. Fu, D. Qin, S. Xie. *Int. J. Electrochem. Sci*., 11 (2016) 577-589.
2. X. Feng, J. Li, L. Lu, J. Hua, L. Xu, M. Ouyang. *J. Power Sources*, 209 (2012) 30-39.
3. T. Bruen, J. Marco. *J. Power Sources*, 310 (2016) 91-101.
4. C. Weng, X. Feng, J. Sun, H. Peng. *Applied Energy*, 180 (2016) 360-368.
5. W. Shi, X. Hu, C. Jin, J. Jiang, Y. Zhang, T. Yip. *J. Power Sources*, 313 (2016) 198-204.
6. M. Dubarry, N. Vuillaume, B.Y. Liaw. *Int. J. Energy Res*., 34 (2010) 216-231.
7. S.F. Schuster, M.J. Brand, P. Berg, M. Gleissenberge, A. Jossen. *J. Power Sources*, 297 (2015) 242-251.
8. Y. Zheng, M. Ouyang, L. Lu, J. Li. *J. Power Sources*, 278 (2015) 287-295.
9. M. Ouyang, X. Feng, X. Han, L. Lu, Z. Li, X. He. *Applied Energy*, 165 (2016) 48-59.
10. L. Zhong, C. Zhang, Y. He, Z. Chen. *Applied Energy*, 113 (2014) 558-564.
11. S. Paul, C. Diegelmann, H. Kabza, W. Tillmetz. *J. Power Sources*, 239 (2013) 642-650.
12. S.J. Harris, D.J. Harris, C. Li. *J. Power Sources*, 342 (2017) 589-597.
13. J. Jiang, C. Zhang. *Fundamentals and application of lithium-ion batteries in electric drive vehicles*. John Wiley & Sons, New York(2015).
14. J. Gallardo-Lozano, E. Romero-Cadaval, M.I. Milanes-Montero, M.A. Guerrero-Martinez. *J. Power Sources*, 246 (2014): 934-949.
15. P. Raspa, L. Frinconi, A. Mancini, M. Cavalletti, S. Longhi, L. Fulimeni, P. Bellesi, R. Isidor. *J. Automotive Safety and Energy*, 2 (2011) 157-164.
16. K. Fang, S. Chen, D. Mu, B. Wu, F. Wu. *J. Power Sources*, 224 (2013) 120-124.
17. J. Zhang, J. Huang, L. Chen, Z. Li. *J. Automotive Safety and Energy*, 5 (2014): 391-400.
18. V. Muenzel, A.F. Hollenkamp, A.I. Bhatt, J. Hoog, M. Brazil, D.A. Thomas, I. Mareels. *J. Electrochem. Soc.*, 162 (2015) A1592-A1600.
19. A. Devie, M. Dubarry. *Batteries*, 2 (2016) 28.
20. H. Dai, Z. Sun, X. Wei, J. Wang. *J. Automotive Safety & Energy*, 1 (2011) 62-67.
21. L. Zhang, S. Wang, Z. Li, H. Deng, Y. Ma, J. Wang. *Int. J. Electrochem. Sci.*, 9 (2014) 6213-6224.
22. Y. Zheng, M. Ouyang, L. Lu, J. Li, X. Han, L. Xu. *J. Power Sources*, 247 (2014) 676-686.
23. Y. Hua, A. Cordoba-Arenas, N. Warner, G. Rizzoni. *J. Power Sources*, 280 (2015) 293-312.
24. D. Andre, M. Meiler, K. Steiner, Ch. Wimmer, T. Soczka-Guth, D.U. Sauer. *J. Power Sources*, 196 (2011) 5334-5341.
25. Y. Liu, L. Song, J. Shen, J. Liu, Z. Xiao. *Int. J. Electrochem. Sci.*, 12 (2017) 1970-1982.
26. S. Miyatake, Y. Susuki, T. Hikihara, S. Itoh, K. Tanaka. *J. Power Sources*, 141 (2013) 736-743.
27. Z. Liu, C. Tan, F. Leng. *Reliability Engineering & System Safety*, 134 (2015) 169-177.